

## Swellable elastomers under constraint

Yucun Lou, Agathe Robisson, Shengqiang Cai, and Zhigang Suo

Citation: *J. Appl. Phys.* **112**, 034906 (2012); doi: 10.1063/1.4745878

View online: <http://dx.doi.org/10.1063/1.4745878>

View Table of Contents: <http://jap.aip.org/resource/1/JAPIAU/v112/i3>

Published by the [American Institute of Physics](#).

---

### Related Articles

Dynamical hysteresis in a self-oscillating polymer gel

*J. Chem. Phys.* **137**, 064103 (2012)

Structural properties of thermoresponsive poly(N-isopropylacrylamide)-poly(ethyleneglycol) microgels

*J. Chem. Phys.* **136**, 214903 (2012)

Instability analysis of a programmed hydrogel plate under swelling

*J. Appl. Phys.* **109**, 063527 (2011)

Effect of the concentration on sol-gel transition of telechelic polyelectrolytes

*J. Chem. Phys.* **134**, 034903 (2011)

Structural changes of poly(N-isopropylacrylamide)-based microgels induced by hydrostatic pressure and temperature studied by small angle neutron scattering

*J. Chem. Phys.* **133**, 034901 (2010)

---

### Additional information on J. Appl. Phys.

Journal Homepage: <http://jap.aip.org/>

Journal Information: [http://jap.aip.org/about/about\\_the\\_journal](http://jap.aip.org/about/about_the_journal)

Top downloads: [http://jap.aip.org/features/most\\_downloaded](http://jap.aip.org/features/most_downloaded)

Information for Authors: <http://jap.aip.org/authors>

## ADVERTISEMENT

**World's Ultimate AFM** Experience the Speed & Resolution



**The fastest AFM on the planet is now simply the best AFM in the world**

[CLICK TO REQUEST INFO](#)

## Swellable elastomers under constraint

Yucun Lou,<sup>1,a)</sup> Agathe Robisson,<sup>1</sup> Shengqiang Cai,<sup>2</sup> and Zhigang Suo<sup>2</sup>

<sup>1</sup>*Schlumberger-Doll Research, One Hampshire Street, Cambridge, Massachusetts 02139, USA*

<sup>2</sup>*School of Engineering and Applied Sciences, Harvard University, Cambridge, Massachusetts 02138, USA*

(Received 13 April 2012; accepted 17 July 2012; published online 13 August 2012)

Swellable elastomers are widely used in the oilfield to seal the flow of downhole fluids. For example, when a crack appears in self-healing cement, the liquid in the surroundings flows into the crack and permeates into the cement, causing small particles of elastomers in the cement to swell, resulting in the blocking of the flow. Elastomers are also used as large components in swellable packers, which can swell and seal zones in the borehole. In these applications, the elastomers swell against the constraint of stiff materials, such as cement, metal, and rock. The pressure generated by the elastomer against the confinement is a key factor that affects the quality of the sealing. This work develops a systematic approach to predict the magnitude of the pressure in such components. Experiments are carried out to determine the stress-stretch curve, free swelling ratio, and confining pressure. The data are interpreted in terms of a modified Flory-Rehner model. © 2012 American Institute of Physics. [<http://dx.doi.org/10.1063/1.4745878>]

### I. INTRODUCTION

Crosslinked polymer networks can absorb solvents and swell many times to their initial volume. Swelling is used by plants to regulate the transport of water,<sup>1</sup> and is exploited in consumer products such as contact lenses<sup>2</sup> and superabsorbent diapers.<sup>3</sup> Swelling elastomers have been developed as vehicles for drug delivery,<sup>4</sup> and as actuators and sensors in microfluidics.<sup>5</sup>

We are particularly interested in the applications of swellable elastomers in the oilfield. During the last decade, the dramatic volume change due to swelling has been widely used in the oilfield to seal undesired fluid flows in the wellbore. Applications include self-healing cements<sup>6–8</sup> and swellable packers.<sup>9–12</sup> The swellable material can seal the fluid channel automatically whenever the fluid is a good solvent, and the types of elastomers can be chosen to respond to certain fluids. For example, a styrene butadiene rubber (SBR) swells in oil while a hydrogel swells in water. Such a seal is self-actuated and requires limited intervention, a feature that is especially attractive in deep wells where intervention is difficult and costly.

In these applications, the swelling of the elastomer is restricted by surrounding materials. In self-healing cements, the swelling of small particles of an elastomer is constrained by the cement. In packers, the swelling of a cylindrical tube of an elastomer is constrained by the casing (a metallic tube) and rocks. The constrained swelling generates a compressive force. In most cases, the larger the swelling-generated force, the better the sealing quality.

Despite the intensive use of swellable materials in the oilfield, an effective method to predict the behavior of swellable elastomers is lacking. A large amount of data has been collected for elastomers under free-swelling conditions, but little work has been done to study elastomers swelling under highly constrained conditions. Nonlinear Flory-type field theories

that are formulated on the basis of kinematics of network deformation, kinetics of solvent migration, and thermodynamics of swelling have been developed in the past few years.<sup>13–16</sup> These theories require few experiments to estimate coefficients values and can be implemented into the commercial finite element software, e.g., ABAQUS, to predict the behavior of swellable elastomer with irregular geometries and under various boundary conditions, which is attractive to the industrial applications. However, more experiments are needed to validate these theories.

This work introduces a systematic approach to analyze swelling elastomers under constraints. This approach combines experiments and modeling. The experimental approach is described first and emphasizes a novel experimental setup that can directly measure the buildup of swelling-induced forces, referred to as swelling pressure. Additional experiments are carried out to measure the stress-stretch curves of an elastomer containing various amounts of solvent, and the swelling ratio under the unconstrained conditions. These data are interpreted by using a modified Flory-Rehner model.

### II. EXPERIMENTS

An oil-swellable elastomer, SBR (23.5% styrene, referenced 1502 at Astlett Rubber), is used to swell in hexadecane ( $C_{16}H_{34}$ ) (99% purity), at 82 °C. This combination can be considered representative of oilfield applications.

Three experiments are used to characterize the swellable elastomer: a uniaxial compression test, a free-swelling test, and a constrained-swelling test. The first two experiments have been extensively used. The third experiment addresses a much less-studied aspect: the constrained-swelling behavior, and was inspired by the work done by Katti and Shanmugasundaram,<sup>17</sup> who measured the swelling pressure of clays.

We perform the uniaxial compression test using samples of various swelling ratios (Fig. 1(a)). Prior to the compression test, the partially swollen samples are prepared and

<sup>a)</sup>Email: [ylou@slb.com](mailto:ylou@slb.com).

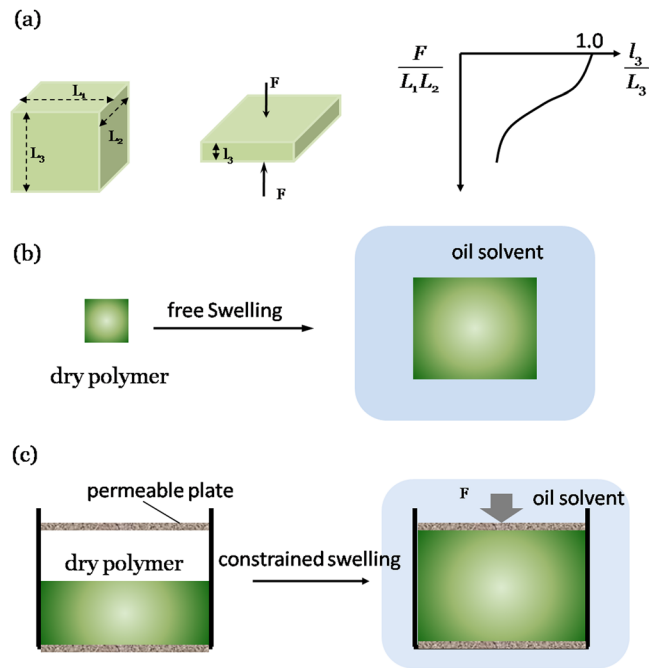


FIG. 1. Schematics of experiments for determining thermodynamics parameters of a gel. (a) Stress-stretch curve measured from uniaxial compression test. (b) Swelling ratio measured from free swelling experiments. (c) Blocking force measured from constrained swelling.

homogenized (swelled samples are wrapped in sealing plastic films and left in oven for homogenization). By fitting the stress-strain response curves with a neo-Hookean model, one can estimate the shear modulus  $G$  of the sample as a function of the swelling ratio.

In the free-swelling test, the sample is submerged in the solvent (Fig. 1(b)). By measuring the volume (or mass) increment as a function of time, one can estimate the kinetics of swelling and the equilibrium volume (or mass) increment of the elastomer.

In the constrained-swelling test, a dry cylindrical sample is placed in a rigid container that has the same radius, preventing the radial swelling (Fig. 1(c)). The sample is placed between two permeable stiff plates with a gap that corresponds to the desired swelling ratio. The whole setup is then heated to the set temperature. Note that the gap needs to be adjusted to take into account any thermal expansion of the setup. Then the solvent is added and the elastomer swells. After the elastomer touches the top surface of the container, it starts generating a force against the top plate. This force builds up over time until it stabilizes. We record the force generated as a function of time by using a load cell. The experiment can be repeated by changing the height of the top plate. This multi-step experiment enables us to plot the equilibrium swelling pressure as a function of swelling ratio, which gives essential information to predict swellable packer sealing ability. Table I lists

TABLE I. Swelling pressure vs. swelling ratio.

$\lambda_c$	1.03	1.10	1.20	1.30	1.40	1.50	1.60	1.70	1.80
$\sigma_3$ (MPa)	5.00	3.15	1.95	1.20	0.75	0.50	0.31	0.19	0.10

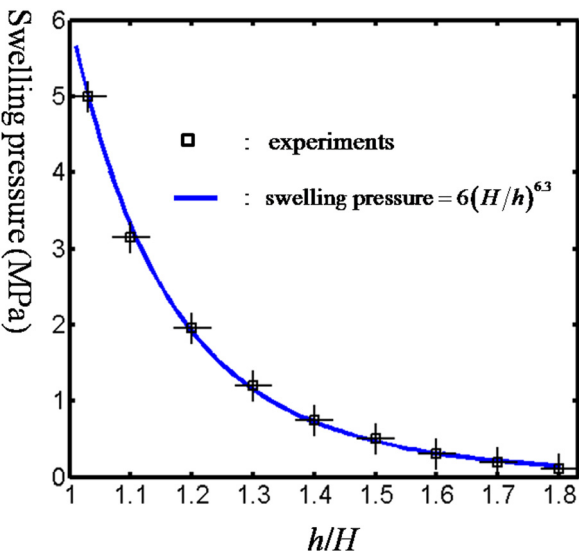


FIG. 2. A power-law data fitting of swelling pressure as a function of swelling ratio for SBR swelling in hexadecane at  $T = 82^\circ\text{C}$ , where the rectangular dots with error bars are experimental results measured via constrained-swelling test. The blue line is the power-law fitting.

the swelling pressures as a function of swelling ratio. Note that the accuracy on setting the swelling ratio is about 3%. As seen in Fig. 2, the experimental results can be fitted with a power-law expression

$$\text{Swelling pressure} = 6.0(H/h)^{6.3}.$$

The exponent value ( $\sim 6.3$ ) obtained here via least-square fitting is larger than the value ( $\sim 1.9$ ) given by Horkay and Zrinyi<sup>18</sup> in the scale theory under semi-dilute condition and the value ( $\sim 2.2$ ) given by Geissler *et al.*<sup>19</sup> via fitting the power-law with polyacrylamide-water gel experiments. Although these types of scaling theories can better match the experimental results than Flory-type theory discussed below (e.g., see Fig. 6), they are difficult to be applied in cases where the elastomer is under complex tri-axial loading and complex boundary conditions.

In this test, the two limiting cases are (1) the zero swelling ratio case, which is to measure the maximum swelling pressure and (2) the maximum swelling ratio with nonzero swelling pressure, which can be used to measure the maximum volume the elastomer can seal under the constrained condition.

It is worth mentioning that the conventional approach to measuring the swelling pressure requires two separate experiments: the first one is to measure the osmotic pressure for uncrosslinked polymer mixed with fluid, and the second one to measure the stress on the crosslinked polymer network under volumetric expansion, referred to as volumetric modulus.<sup>20</sup> The swelling pressure becomes the difference between osmotic pressure and volumetric modulus. This method is applicable for pure systems only and requires the detailed knowledge of the swellable elastomer, which is either not available in many industrial applications when the material is a trade secret, or too complex (elastomers can be blended with ten or more additives).

### III. THEORY

In this section, a modified Flory-Rehner model is introduced as an extension of our previous work.<sup>21</sup> Consider a block of representative volume of elastomer (Fig. 3). In the reference state, the block is a dry network and subject to no stresses, and is of dimensions  $L_1$ ,  $L_2$ , and  $L_3$ . When submerged in a solvent-containing environment and subjected to forces  $P_1$ ,  $P_2$ , and  $P_3$ , the block absorbs  $\Sigma$  number of solvent molecules and is of dimensions  $l_1$ ,  $l_2$ , and  $l_3$ . Let  $\Omega$  be the volume per solvent molecule. If we assume that both elastomers and solvents are incompressible, the volume in current state  $V \equiv l_1 l_2 l_3$  equals the sum of the volume of the dry network  $V_0 \equiv L_1 L_2 L_3$  and the volume of absorbed solvent molecules  $\Omega \Sigma$

$$l_1 l_2 l_3 = L_1 L_2 L_3 + \Omega \Sigma. \quad (1)$$

Define the nominal concentration of solvent by  $C = \Sigma/V_0$ , and the stretches by  $\lambda_1 = l_1/L_1$ ,  $\lambda_2 = l_2/L_2$ , and  $\lambda_3 = l_3/L_3$ . Equation (1) can be written as

$$\lambda_1 \lambda_2 \lambda_3 = 1 + \Omega C = V/V_0. \quad (2)$$

Let  $\mu$  be the chemical potential of the solvent in the environment, and  $W$  be the free energy of the block in the current state divided by the volume of the block in the reference state. Define the stresses as  $\sigma_1 = P_1/(l_2 l_3)$ ,  $\sigma_2 = P_2/(l_3 l_1)$ , and  $\sigma_3 = P_3/(l_1 l_2)$ . When the network equilibrates with the environment and the applied forces, the stresses are given by<sup>15,21</sup>

$$\sigma_1 = \frac{\partial W(\lambda_1, \lambda_2, \lambda_3)}{\lambda_2 \lambda_3 \partial \lambda_1} - \frac{\mu}{\Omega}, \quad (3)$$

$$\sigma_2 = \frac{\partial W(\lambda_1, \lambda_2, \lambda_3)}{\lambda_1 \lambda_3 \partial \lambda_2} - \frac{\mu}{\Omega}, \quad (4)$$

$$\sigma_3 = \frac{\partial W(\lambda_1, \lambda_2, \lambda_3)}{\lambda_1 \lambda_2 \partial \lambda_3} - \frac{\mu}{\Omega}. \quad (5)$$

Following the classical work of Flory and Rehner,<sup>22</sup> we assume that the change in the free energy during swelling is a sum of elastic and mixing energy

$$W = W_{\text{elastic}} + W_{\text{mix}}. \quad (6)$$

The elastic energy is described by the neo-Hookean model, leading to the scaling relation<sup>21</sup>

$$\tilde{G}^F = G_0 (V/V_0)^{-1/3}, \quad (7)$$

where  $V_0$  is the volume and  $G_0$  is the shear modulus of the dry elastomer, and  $V$  is the volume and  $\tilde{G}^F$  is the shear modulus of the swollen elastomer. As shown below, the scaling relation (7) does not fit our experimental data. Note that the scaling relation (7) was challenged by De Gennes,<sup>23</sup> who showed that in many instances, both the elastic and the entropic energies were largely overestimated in the Flory-Rehner model. A dependence in  $(V/V_0)^{-7/12}$  (Ref. 24) was reported. Here, we modify the expression (7), and write that the shear modulus at the current configuration denoted as  $\tilde{G}^M$ , as

$$\tilde{G}^M = G_0 (V/V_0)^{-\alpha-1/3} = G_m (V/V_0)^{-1/3}, \quad (8)$$

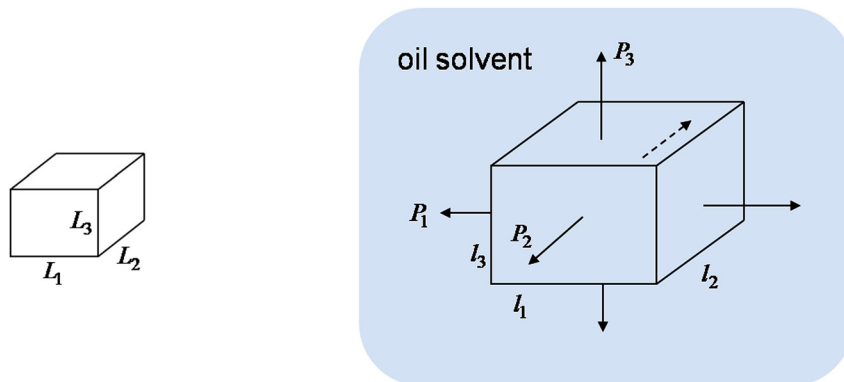
where a parameter  $\alpha$  is introduced to account for the variation of the shear modulus with swelling ratio. We define  $G_m \equiv G_0 (V/V_0)^{-\alpha}$  as the shear modulus variation in addition to the volumetric effect considered by Flory and Rehner. Using this modified shear modulus, we write the elastic energy density in the form of neo-Hookean model

$$W_{\text{elastic}} = \frac{G_m(\lambda_1 \lambda_2 \lambda_3, \alpha)}{2} [\lambda_1^2 + \lambda_2^2 + \lambda_3^2 - 3 - 2 \log(\lambda_1 \lambda_2 \lambda_3)]. \quad (9)$$

The mixing energy is approximated using a modified version of Flory-Huggins model<sup>25,26</sup>

$$W_{\text{mix}} = k_B T \left[ \beta C \log \frac{\Omega C}{1 + \Omega C} + \frac{\chi C}{1 + \Omega C} \right], \quad (10)$$

where  $\beta$  is a dimensionless parameter and  $\chi$  is the Flory-Huggins parameter that measures the interaction between the elastomer and solvent. The first and second terms in the bracket are the contribution of entropy and enthalpy to the mixing, respectively. The parameter  $\beta$  is introduced following the work of Lichtenthaler *et al.*<sup>25</sup> who have shown that the Flory-Huggins model overestimates the entropy of swelling if there is a size difference between species.



(a) Referenced State (dry network)

(b) Current State

FIG. 3. (a) In the reference state, a dry network of polymers contains no oil and is subject to no applied forces. (b) In the current state, the network is in equilibrium with applied forces, and with an environment in which the chemical potential of the oil is fixed.



A combination of Eqs. (2)–(10) gives

$$\frac{\sigma_1 \Omega}{k_B T} = \frac{G_m}{\lambda_1 \lambda_2 \lambda_3} \left[ \left( 1 - \frac{1}{\lambda_1^2} \right) - \frac{\alpha}{2} N(\lambda_1, \lambda_2, \lambda_3) \right] + \beta \log \left( 1 - \frac{1}{\lambda_1 \lambda_2 \lambda_3} \right) + \frac{\beta}{\lambda_1 \lambda_2 \lambda_3} + \frac{\chi}{\lambda_1^2 \lambda_2^2 \lambda_3^2} - \frac{\mu}{\Omega}, \quad (11)$$

$$\frac{\sigma_2 \Omega}{k_B T} = \frac{G_m}{\lambda_1 \lambda_2 \lambda_3} \left[ \left( 1 - \frac{1}{\lambda_2^2} \right) - \frac{\alpha}{2} N(\lambda_1, \lambda_2, \lambda_3) \right] + \beta \log \left( 1 - \frac{1}{\lambda_1 \lambda_2 \lambda_3} \right) + \frac{\beta}{\lambda_1 \lambda_2 \lambda_3} + \frac{\chi}{\lambda_1^2 \lambda_2^2 \lambda_3^2} - \frac{\mu}{\Omega}, \quad (12)$$

$$\frac{\sigma_3 \Omega}{k_B T} = \frac{G_m}{\lambda_1 \lambda_2 \lambda_3} \left[ \left( 1 - \frac{1}{\lambda_3^2} \right) - \frac{\alpha}{2} N(\lambda_1, \lambda_2, \lambda_3) \right] + \beta \log \left( 1 - \frac{1}{\lambda_1 \lambda_2 \lambda_3} \right) + \frac{\beta}{\lambda_1 \lambda_2 \lambda_3} + \frac{\chi}{\lambda_1^2 \lambda_2^2 \lambda_3^2} - \frac{\mu}{\Omega}, \quad (13)$$

where  $N(\lambda_1, \lambda_2, \lambda_3)$  is given by

$$N(\lambda_1, \lambda_2, \lambda_3) = \lambda_1^2 + \lambda_2^2 + \lambda_3^2 - 3 - 2 \log(\lambda_1 \lambda_2 \lambda_3).$$

Note that these expressions are identical to those given in the work done by Hong *et al.*<sup>15</sup> when  $\alpha = 0$  and  $\beta = 1$ .

#### IV. PARAMETERS ESTIMATION AND MODEL VALIDATION

The modified Flory-Rehner model introduces the following parameters:  $\Omega$ ,  $G_o$ ,  $\alpha$ ,  $\beta$ , and  $\chi$ . The molecular volume of hexadecane is known,  $\Omega = 5.15 \times 10^{-28} \text{ m}^3$ . The initial shear modulus of dried elastomer,  $G_o$ , is estimated as 0.7 MPa by fitting the stress-strain curve measured via uniaxial compression test (Fig. 4). The shear moduli of samples of various swelling ratios are measured with the same method (Fig. 5). We use these experimental results to estimate  $\alpha$  in the expression (8) with adopting the least square fitting method and estimate  $\alpha = 0.47$ . (Note that the standard deviation for this fitting is 5%.)

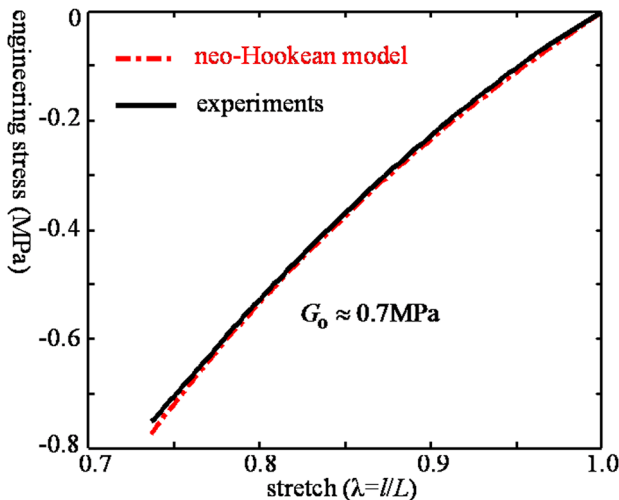


FIG. 4. Stress-stretch curves measured via uniaxial-compression test (solid line) and the numerical fitting using the neo-Hookean model. The shear modulus of dried SBR is estimated to be  $G_o = 0.7 \text{ MPa}$ .

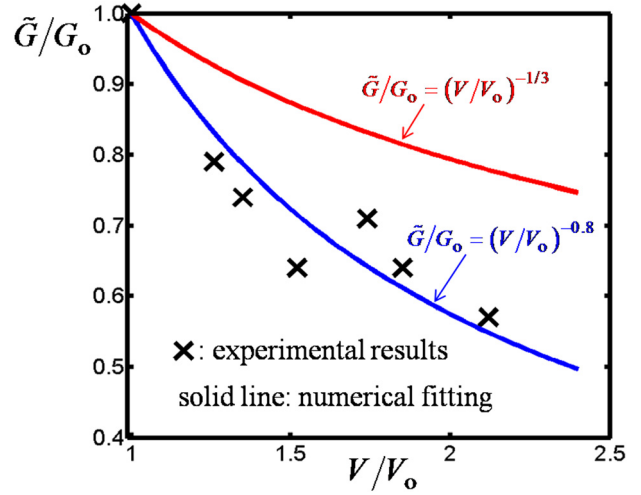


FIG. 5. The drop of shear modulus with respect to swelling. The shear modulus of swelled samples (x in the figure) is measured via uniaxial compression test.

The other two coefficients  $\beta$  and  $\chi$  are estimated using a combination of the free-swelling test and one step of the multi-step constrained-swelling test. In the free-swelling test, the principal stretches of the elastomer sample are equal in each direction at equilibrium. Equation (1) gives that

$$\lambda_1 = \lambda_2 = \lambda_3 = \lambda_f = (1 + \Omega C)^{1/3} = (V/V_o)^{1/3}. \quad (14)$$

For SBR swelling in hexadecane at  $82^\circ \text{C}$ , we have measured the equilibrium volume expansion,  $V/V_o \approx 210\%$ , so that  $\lambda_f \approx 1.3$ .

When an elastomer swells in a pure solvent under no constraint, in equilibrium, the stresses and the chemical potential vanish

$$\sigma_1 = \sigma_2 = \sigma_3 = 0, \quad \mu = 0. \quad (15)$$

Inserting Eq. (15) into Eq. (11), we obtain that

$$\frac{G_m \Omega}{k_B T} \left[ \left( \frac{1}{\lambda_f^2} - \frac{3\alpha}{2} \right) \left( \lambda_f - \frac{1}{\lambda_f} \right) + \frac{3\alpha}{\lambda_f} \log \lambda_f \right] + \beta \log \left( 1 - \frac{1}{\lambda_f^3} \right) + \frac{\beta}{\lambda_f^3} + \frac{\chi}{\lambda_f^6} = 0. \quad (16)$$

In the constrained-swelling test, the stretches along the radial and circumferential directions are constrained

$$\lambda_1 = \lambda_2 \approx 1. \quad (17)$$

The only deformation is along the axial direction, and is controlled by the height of the top surface. For a sample with initial thickness  $H$  swelling in a container with height  $h$ , the stretches along the axial direction are uniform in equilibrium, which is given by

$$\lambda_3 = \lambda_c = h/H. \quad (18)$$

By substituting Eqs. (17) and (18) into Eq. (13), we obtain

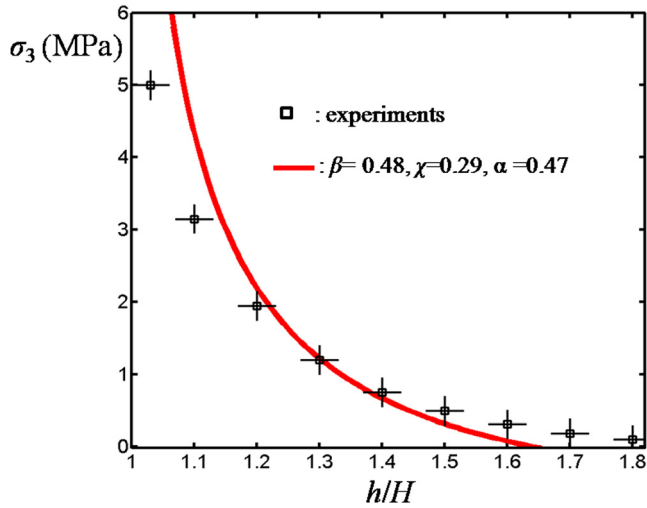


FIG. 6. Comparison between simulations and experiments for SBR to swell in hexadecane at  $T = 82^\circ\text{C}$ , where the rectangular dots with error bars are experimental results measured via constrained-swelling test. The red line is the modeling results.

$$\frac{\sigma_3 \Omega}{k_B T} = \frac{G_m \Omega}{k_B T} \left[ \left(1 - \frac{\alpha}{2}\right) \left(\lambda_c - \frac{1}{\lambda_c}\right) + \frac{\alpha \log \lambda_3}{\lambda_c} \right] + \beta \log(\lambda_c - 1) + \frac{\beta}{\lambda_c} + \frac{\chi}{\lambda_c^2}. \quad (19)$$

For example, in the fourth step of the confined swelling experiment, as listed in Table I,  $\lambda_c = 1.3$  and  $\sigma_3 = 0.5$  MPa. By solving Eqs. (16) and (19) with the experimental data mentioned above, we can estimate the values of coefficients  $\chi$  and  $\beta$

$$\chi = 0.29 \quad \text{and} \quad \beta = 0.48. \quad (20)$$

From matching with the experimental results, one sees that the entropy of mixing is only about 50% of that predicted by the original Flory-Huggins theory.

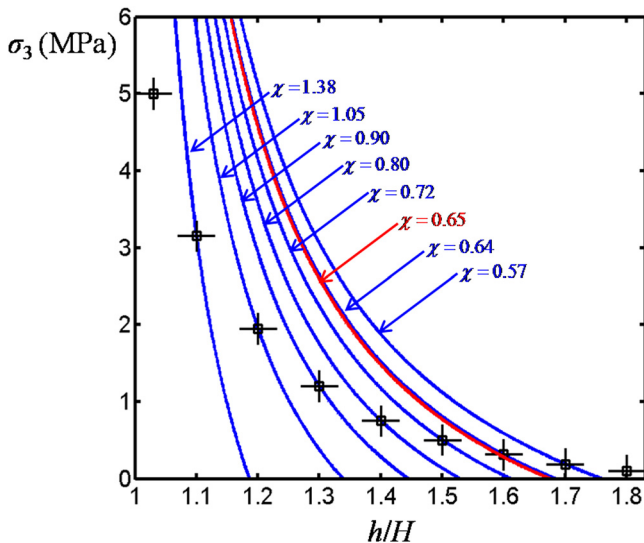


FIG. 7. Comparison between simulations by taking  $\alpha = 0$  and  $\beta = 1$  and experiments for SBR to swell in hexadecane at  $T = 82^\circ\text{C}$ . The values of  $\chi$  are estimated via one of the constrained-swelling test in blue line and via the free-swelling test in red line.

Finally, the model can be validated by comparing with the data obtained from all steps in the multi-step constrained swelling test (Fig. 6). The modeling results are in good agreement with experiments in a relatively large range, i.e.,  $1.2 < \lambda_c < 1.6$ . As a comparison, if we neglect the effect of swelling on shear modulus and the modification of entropy term ( $\alpha = 0$  and  $\beta = 1$ ), the coefficient value of  $\chi$  can be estimated via the free-swelling test result using Eq. (16) or one step of the constrained-swelling test using Eq. (19). None of these curves match the experiments (Fig. 7). In addition, if we chose to vary the coefficient  $\chi$  with the swelling ratio to match the confined swelling tests, then the values of  $\chi$  would be doubled from  $\lambda_c = 1.7$  ( $\chi = 0.57$ ) to  $\lambda_c = 1.2$  ( $\chi = 1.38$ ). Although this procedure is commonly practiced to fit the Flory-Huggins model to experimental data,<sup>27</sup> we do not pursue it here.

## V. CONCLUSIONS

The swelling pressure generated by the elastomer under geometrical constraints, which is the essential for the sealing applications, has been studied systematically through both experiments and numerical simulations. The experimental method developed in this work, i.e., the multi-step constrained-swelling test, can directly measure the swelling pressure generated by an elastomer in solvent without requiring any knowledge of the composition of the elastomer. In the field theory developed in this work, the variation of elastic modulus with swelling and the modification of entropy of mixing relative to the initial Flory-Huggins theory have been considered and shown to be important on the stiff elastomer swelling in organic solvent. The theoretical predictions are validated via comparing with experimental results and consistency is observed both theory and experiments.

## ACKNOWLEDGMENTS

The work at Harvard was supported by MRSEC and by Schlumberger.

- <sup>1</sup>M. A. Zwieniecki, P. J. Melcher, and N. M. Holbrook, *Science* **291**, 1059 (2001).
- <sup>2</sup>M. F. Refojo, in *Biomaterials Science*, edited by B. D. Ratner, A. S. Hoffman, F. J. Schoen, and J. E. Lemons (Elsevier, Boston, 2004), pp. 583–590.
- <sup>3</sup>F. Masuda, in *Superabsorbent Polymers*, edited by F. L. Buchholtz and N. A. Peppas (American Chemical Society, Washington, D.C., 1994), pp. 88–89.
- <sup>4</sup>R. Langer, *Nature* **392**, 5 (1998).
- <sup>5</sup>A. Richter, S. Howitz, D. Kuckling, and K. F. Amdt, *Sens. Actuators B* **99**, 451 (2004).
- <sup>6</sup>P. Cavanagh, C. R. Johnson, S. LeRoy-Delage, G. DeBruijn, I. Cooper, D. Guillot, H. Bulte, and B. Dargaud, in *SPE/IADC Drilling Conference*, Amsterdam, The Netherlands, 20–22 February 2007, Paper No. SPE/IADC 105781.
- <sup>7</sup>N. Moroni, N. Panciera, A. Zanchi, C. R. Johnson, S. LeRoy-Delage, H. Bulte-Loyer, S. Cantini, and E. Belleggia, in *SPE Annual Technical Conference and Exhibition*, Anaheim, California, US., 11–14 November 2007, Paper No. SPE 110523.
- <sup>8</sup>J. Roth, C. Reeves, C. R. Johnson, G. De Bruijn, M. Bellalarba, S. LeRoy-Delage, and H. Bulte-Loyer, in *IADC/SPE Drilling Conference*, Orlando, Florida, US., 4–6 March 2008, Paper No. IADC/SPE 112715.
- <sup>9</sup>M. Kleverlaan, R. H. van Noort, and I. Jones, in *SPE/IADC Drilling Conference*, Amsterdam, The Netherlands, 23–25 February 2005, Paper No. SPE/IADC 92346.
- <sup>10</sup>V. Fjellstad, R. Berbkvam, and T. Li, *Hart's E&P* **79**, 79 (2006).

- <sup>11</sup>M. S. Laws, J. E. Fraser, H. F. Soek, and N. Carter, in *Asia Pacific Drilling Conference and Exhibition*, Bangkok, Thailand, 13–15 November 2006, Paper No. IADC/SPE 100361.
- <sup>12</sup>D. Hembling, S. Salamy, A. Qatani, N. Carter, and S. Jacob, in *Drilling Contractor*, September/October, 2007, pp. 108–114.
- <sup>13</sup>M. Doi, *J. Phys. Soc. Jpn.* **78**, 052001 (2009).
- <sup>14</sup>S. A. Chester and L. Anand, *J. Mech. Phys. Solids* **58**, 1879 (2010).
- <sup>15</sup>W. Hong, X. H. Zhao, J. X. Zhou, and Z. G. Suo, *J. Mech. Phys. Solids* **56**, 1779 (2008).
- <sup>16</sup>W. Hong, Z. S. Liu, and Z. G. Suo, *Int. J. Solids Struct.* **46**, 3282 (2009).
- <sup>17</sup>D. R. Katti and V. Shanmugasundaram, *Can. Geotech. J.* **38**, 175 (2001).
- <sup>18</sup>F. Horkay and M. Zrinyi, *Macromolecules* **15**, 1306 (1982).
- <sup>19</sup>E. Geissler, A.-M. Hecht, F. Horkay, and M. Zrinyi, *Macromolecules* **21**, 2594 (1988).
- <sup>20</sup>M. Rubinstein, R. H. Colby, A. V. Dobrynin, and J.-F. Joanny, *Macromolecules* **29**, 398 (1996).
- <sup>21</sup>S. Cai, Y. Lou, A. Robisson, P. Ganguly, and Z. Suo, *J. Appl. Phys.* **107**, 103535 (2010).
- <sup>22</sup>P. J. Flory and J. Rehner, *J. Chem. Phys.* **11**, 521 (1943).
- <sup>23</sup>P.-G. De Gennes, *Scaling Concepts in Polymer Physics*, 1st ed. (Cornell University Press, 1979), pp 46–47.
- <sup>24</sup>S. P. Obukhov, M. Rubinstein, and R. H. Colby, *Macromolecules* **27**, 3191 (1994).
- <sup>25</sup>R. N. Lichtenthaler, D. S. Abrams, and J. M. Prausnitz, *Can. J. Chem.* **51**, 3071 (1973).
- <sup>26</sup>A. Vetere, *Fluid Phase Equilib.* **34**, 21 (1987).
- <sup>27</sup>B. Xu, X. Di, and G. B. McKenna, *Macromolecules* **45**, 2402 (2012).